

## Understanding the nature of baryon resonances

DEREK B. LEINWEBER<sup>(1)</sup>, CURTIS D. ABELL<sup>(1)</sup>, LIAM C. HOCKLEY<sup>(1)</sup>,  
WASEEM KAMLEH<sup>(1)</sup>, ZHAN-WEI LIU<sup>(2)</sup><sup>(3)</sup><sup>(4)</sup>, FINN M. STOKES<sup>(1)</sup><sup>(5)</sup>,  
ANTHONY W. THOMAS<sup>(1)</sup> and JIA-JUN WU<sup>(6)</sup><sup>(7)</sup>

<sup>(1)</sup> *Special Research Centre for the Subatomic Structure of Matter (CSSM), Department of Physics, University of Adelaide - Adelaide, South Australia 5005, Australia*

<sup>(2)</sup> *School of Physical Science and Technology, Lanzhou University - Lanzhou 730000, China*

<sup>(3)</sup> *Research Centre for Hadron and CSR Physics, Lanzhou University and Institute of Modern Physics of CAS - Lanzhou 730000, China*

<sup>(4)</sup> *Lanzhou Center for Theoretical Physics, Key Laboratory of Theoretical Physics of Gansu Province, Key Laboratory of Quantum Theory and Applications of MoE, and Frontiers Science Center for Rare Isotopes, Lanzhou University - Lanzhou 730000, China*

<sup>(5)</sup> *Jülich Supercomputing Centre, Forschungszentrum Jülich - D-52428 Jülich, Germany*

<sup>(6)</sup> *School of Physical Sciences, University of Chinese Academy of Sciences (UCAS) Beijing 100049, China*

<sup>(7)</sup> *Southern Center for Nuclear-Science Theory (SCNT), Institute of Modern Physics, Chinese Academy of Sciences - Huizhou 516000, Guangdong Province, China*

received 21 December 2023

**Summary.** — This paper opens with a brief review of lattice QCD calculations showing the  $2s$  radial excitation of the nucleon sits at approximately 2 GeV, well above the Roper resonance position. We then proceed to reconcile this observation with experimental scattering data. While the idea of dressing quark-model states in a coupled-channel analysis to describe scattering data has been around for decades, it is now possible to bring these descriptions to the finite volume of lattice QCD for confrontation with lattice-QCD calculations. This combination of lattice QCD and experiment demands that we reconsider our preconceived notions about the quark model and its excitation spectrum. We close with a discussion of an unanticipated resolution to the missing baryon resonances problem.

### 1. – Introduction

Perhaps the most surprising and unanticipated discovery in low-lying baryon spectroscopy is the discovery that the  $2s$  radial excitation of the nucleon lies at approximately 2 GeV [1-12], far from the Roper resonance of the nucleon at 1.44 GeV [13]. So ingrained is the idea that the Roper resonance is associated with the  $2s$  excitation of the simple quark model, the literature even refers to the  $2s$  quark-model excitation as the Roper state. We now know this is not the case.

Remarkably the idea that the  $\Lambda(1405)$  resonance is not a quark-model state [14, 15] is widely accepted. Here even the two-pole structure associated with attractive coupled-channel effects in the  $\pi\Sigma$  and  $\bar{K}N$  channels is understood [16-18].

However, this is not necessarily the case for the Roper resonance. Nevertheless, the Roper resonance should now be understood to be generated by rescattering in the coupled channels of  $\pi N$ ,  $\sigma N$ , and  $\pi\Delta$ . Here the  $\sigma N$ , and  $\pi\Delta$  channels are the resonant contributions from the three-body  $\pi\pi N$  channel.

In the following section, we briefly review the lattice QCD calculations revealing that the radial excitation of the nucleon sits at 2 GeV. Attempts to find more exotic descriptions of the Roper resonance in lattice QCD are also reviewed in sect. 2.

With the radial excitation entrenched at 2 GeV, analysis turns to the  $\pi N$  phase shift data, exploring whether one can describe this data without a low-lying radial excitation near the Roper resonance. Here Hamiltonian Effective Field Theory is used to bring the scattering data of experiment to the finite volume of lattice QCD to confront the results of contemporary lattice QCD calculations. This research is briefly reviewed in sect. 3.

These discoveries provide a novel and unanticipated resolution of the long-standing missing baryon resonances problem and this solution is presented in the closing section.

## 2. – Lattice QCD

The first hint that there was a problem with the excitation energy of the  $2s$  radial excitation of the nucleon in full  $2+1$  flavour lattice QCD [19] was reported in the preprint of ref. [1]. By using superpositions of Gaussian-shaped smeared quark sources, this work presents the first attempt to excite the  $2s$  radial excitation of the nucleon in full QCD.

By combining narrow and wide Gaussian sources with opposite signs, one can create a node in the wave function of the quark distributions within the nucleon. The well-established generalised eigenvalue solution [20, 21] is employed to calculate the manner in which the Gaussian-smeared quark sources are superposed to create the  $2s$  radial excitation on the lattice.

Figure 3 of ref. [1] illustrates the invariance of the  $2s$  excitation energy obtained. It was impossible to generate a low-lying  $2s$  excitation. These results were subsequently confirmed by the HSC Collaboration at heavy quark masses [22] and others [2, 3]. A consensus began to emerge in 2015 [4] particularly with the advent of the Athens Model-Independent Analysis Scheme [3]. The wave functions of both the  $2s$  and  $3s$  excitations were directly calculated in lattice QCD [5, 6] and their profiles compare well with the expectations of a constituent quark model [5].

More exotic five-quark descriptions for the Roper resonance were pursued in refs. [7, 8]. However, no new low-lying states were observed. Similarly the consideration of hybrid baryons [9] did not reveal any new low-lying states in the Roper channel.

Next-generation calculations appeared in 2016 with a high-statistics calculation coming from the CSSM [10] and the very first insights of the role of two-particle scattering states from Lang *et al.* [11]. Here the three-quark-dominated state continued to be observed at  $\sim 2$  GeV, confirming earlier observations [1-8], even when lower-lying scattering states are included in the correlation matrix.

The role of chiral symmetry in lattice fermion actions was explored quantitatively in ref. [23] to see if the explicit breaking of chiral symmetry in Wilson-clover fermion actions was responsible for the large  $2s$  excitation energy. A direct analysis of lattice correlation functions from Wilson-clover and overlap fermion actions—the latter providing a lattice implementation of chiral symmetry—revealed no differences in the spectrum.

Since then, parity-expanded variational analysis (PEVA) techniques [24] have been developed to explore the electromagnetic form factors of both the even- and odd-parity excitations of the nucleon [12] and their electromagnetic transitions to the ground state [25].

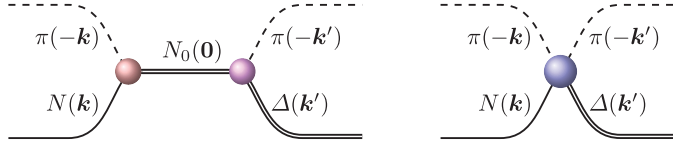


Fig. 1. – Examples of one-to-two (left) and two-to-two (right) vertices contributing to  $\pi N$  scattering in the rest frame. Here  $N_0$  denotes the single-particle  $2s$  radial excitation of the nucleon.

With regard to the  $2s$  excitation, the charge radius of the excited proton is larger than the ground state, in accord with expectations. Moreover, the magnetic moments of the excited  $2s$  proton and neutron calculated in lattice QCD agree with the ground-state magnetic moments, again consistent with the expectations of a  $2s$  excitation.

The most recent calculations of the nucleon spectrum are focused on the lowest-lying scattering states [18,26-28]. As described in detail in the next section, these energy levels are consistent with  $\pi N$  scattering data from experiment, providing confidence in their world-leading computationally challenging analysis methods.

In summary, there is overwhelming evidence that the  $2s$  radial excitation of the nucleon has been observed in lattice QCD. On a lattice volume of 3 fm on a side, the state sits at 1.9(1) GeV. One then naturally asks, is this result even consistent with experiment? It is possible to describe  $\pi N$  scattering data in the absence of a low-lying single-particle quark-model state. If so, then what is the Roper resonance?

### 3. – Hamiltonian effective field theory

**3.1. Infinite volume.** – The idea of dressing quark-model states in a coupled-channel analysis to describe scattering data has been around for decades [29]. However, recent advances in understanding the nature of baryon excitations are flowing from the novel ability to bring these coupled-channel descriptions to the finite volume of lattice QCD for confrontation with lattice-QCD calculations. This combination of lattice QCD and experiment demands that we reconsider our preconceived notions about the quark model and its excitation spectrum.

Herein, the infinite-volume world of experiment and the finite-volume world of lattice QCD are bridged by Hamiltonian effective field theory (HEFT), a non-perturbative extension of effective field theory incorporating the Lüscher formalism [30,31]. HEFT calculations typically commence in infinite volume with the aim to describe experimental scattering data [10,32-36]. Single and non-interacting two-particle states mix via one-to-two and two-to-two vertices as depicted in fig. 1.

The functional form of the one-to-two vertices are governed by heavy-baryon chiral perturbation theory [31,34] and the two-to-two vertices are described by separable potentials which facilitate a closed-form solution of the standard coupled-channel equations [35]. Here the potentials become phenomenological, adopting a momentum dependence as demanded by the scattering data [32]. Remarkably, the Lüscher formalism embedded within HEFT ensures the low-lying finite-volume spectrum is independent of the phenomenology used to describe the data, provided the data is described accurately [34].

Of course HEFT can be used in the more traditional manner where lattice QCD results constrain the Hamiltonian and infinite-volume scattering observables are predicted [37,38]. In the baryon sector, there is a lack of precision results showing the subtle shifts of the non-interacting spectra due to the finite volume of the lattice. It is better to bring

the precision experimental scattering data to the finite volume of lattice QCD.

As one moves up in the spectrum, more coupled channels come into effect. Reference to the partial decay widths of the resonances under investigation can inform the essential channels to be included in the calculation. For example, the  $\pi N$ ,  $\sigma N$  and  $\pi\Delta$  channels are all observed in the partial decay widths of the Roper resonance making their inclusion essential to understanding the structure of the Roper resonance. In the absence of experimental analyses of the  $\pi N$  to  $\pi\Delta$  and  $\sigma N$  scattering amplitudes, there is insufficient information to uniquely constrain the Hamiltonian from experimental data alone.

As a result, fits to the experimental data provide a variety of Hamiltonians, all describing the experimental  $\pi N$  phase shift and inelasticity but describing the composition of the spectrum in a different manner. It is here, that the finite-volume predictions of the various coupled-channel fits can be confronted with lattice QCD results.

**3.2. Finite volume.** – In going from infinite volume to finite volume, the continuum of momentum states becomes quantised to the momenta available on a finite periodic volume. Scattering potentials constrained by experiment pick up finite-volume factors and form the elements of a matrix Hamiltonian. One then solves the Schrödinger equation

$$(1) \quad \langle i | H | j \rangle \langle j | E_\alpha \rangle = E_\alpha \langle i | E_\alpha \rangle,$$

where  $|i\rangle$  and  $|j\rangle$  are the non-interacting basis states taking the discrete momenta available on the periodic volume (*e.g.*,  $|\pi(\mathbf{k})N(-\mathbf{k})\rangle$ ),  $E_\alpha$  is the energy eigenvalue for the finite-volume energy eigenstate labelled by  $\alpha$ , and  $\langle i | E_\alpha \rangle$  is the eigenvector of the Hamiltonian matrix  $\langle i | H | j \rangle$  describing the composition of the finite-volume energy eigenstate  $\alpha$  in terms of the non-interacting basis states  $|i\rangle$ .

The ability of HEFT to describe the pion mass dependence of the finite-volume energy eigenstates and provide a description of their composition is key to the advances being made. Of particular importance is the contribution of the single-particle basis state to the energy eigenstates. As analyses of the nucleon spectrum in the excitation regime of the Roper are performed with local three-quark interpolating fields, the overlap of the single-particle basis state  $|N_0\rangle$  with the energy eigenstate  $|\alpha\rangle$  provides information of the energy eigenstates most likely to be excited in lattice QCD calculations.

More quantitatively, Bär *et al.* [39] provided a  $\chi$ PT estimate of the coupling between a smeared nucleon interpolating field and a non-interacting pion-nucleon basis state

$$(2) \quad \frac{3}{16} \frac{1}{(f_\pi L)^2 E_\pi L} \left( \frac{E_N - m_N}{E_N} \right) \approx 10^{-3},$$

where  $E_\pi$  and  $E_N$  are on-shell pion and nucleon energies. The numerical estimate is based on a 3 fm lattice and the lowest non-trivial momentum contribution where the coupling is largest. Here the  $1/L^3$  dependence of the coupling is manifest as the non-interacting two-particle momentum state is spread uniformly throughout the lattice volume.

Noting the small magnitude of the overlap between the local interpolating field and the two-particle basis states, one concludes that the state excited by the local interpolating field is the only local state in the Hamiltonian basis, the single-particle basis state,  $|N_0\rangle$ . Thus, we associate the three-quark nucleon interpolating field  $\bar{\chi}$  acting on the QCD vacuum,  $|\Omega\rangle$ , with the bare  $2s$ -nucleon basis state of HEFT, via  $\bar{\chi}(0)|\Omega\rangle = |N_0\rangle$ . The most likely energy eigenstate to be observed in lattice QCD is the energy eigenstate having the largest overlap with  $|N_0\rangle$  as indicated by a survey of  $\langle N_0 | E_\alpha \rangle$  over  $\alpha$ .

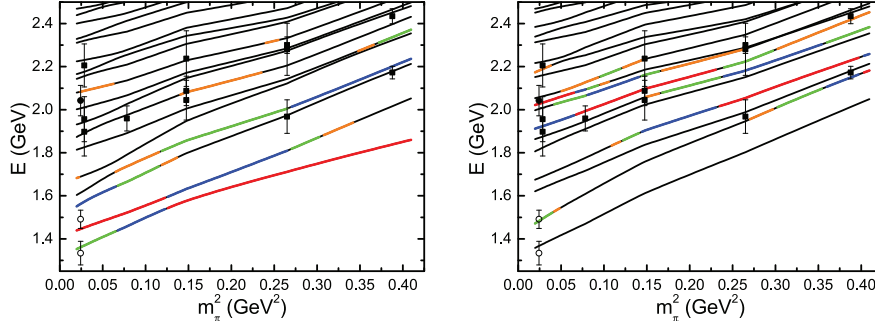


Fig. 2. – The finite-volume spectra predicted by HEFT [33] (solid lines) for a lattice QCD volume of  $(3 \text{ fm})^3$  are confronted with results from lattice QCD (bullets and squares). The left plot is the familiar scenario with  $m_0 = 1.7 \text{ GeV}$  and the right-hand plot has  $m_0 = 2.0 \text{ GeV}$ . Line colours illustrate the energy eigenstates with the largest quark-model single-particle components in the order red, blue, green, and orange. These are the most likely states to be excited with local three-quark interpolating fields in lattice QCD. Bullets indicate the lattice results from Lang *et al.* [11] and squares are from the CSSM [10]. Open symbols denote energy eigenstates dominated by two-particle momentum projected interpolating fields and full symbols denote energy eigenstates dominated by local three-quark interpolating fields.

Remarkably, there is sufficient information in the eigenvectors of HEFT to actually simulate what lattice QCD correlation functions of three-quark operators look like

$$(3) \quad G_{N_0}(t) = \sum_i |\langle N_0 | E_i \rangle|^2 e^{-E_i t}.$$

This was examined in ref. [35] and the favourable comparison with lattice QCD results is noteworthy.

**3.3. Confrontation with lattice QCD.** – Noting that experimental  $\pi N$  scattering data alone is not enough to uniquely constrain the Hamiltonian, we bring the coupled-channel predictions to the finite volume of lattice QCD to confront the predictions with lattice QCD determinations of the mass spectrum.

Of critical importance is where the states excited by local three-quark interpolating fields lie in the spectrum. HEFT predicts not only the positions of the energy eigenstates but also their composition. A careful comparison of the composition in HEFT with the interpolating fields used to excite the states in lattice QCD is very powerful in discriminating between various descriptions of the experimental scattering data. To be clear, all coupled-channel analyses considered herein describe the experimental  $\pi N$  scattering data well and generate poles in the complex plane in agreement with the Particle Data Group [40].

To differentiate between the many possible descriptions of experimental data alone, we label two fits of interest by the bare mass,  $m_0$ , of the single-particle state associated with the  $2s$  radial excitation of the quark model, namely  $m_0 = 1.7 \text{ GeV}$  and  $m_0 = 2.0 \text{ GeV}$ . The former value leads to the familiar scenario where the quark-model state is dressed by meson-baryon states to lie in the regime of the Roper resonance.

The excellent description of the  $\pi N$  scattering data for both of these scenarios is presented in fig. 1 of ref. [33] where there is very little to differentiate between the two fits. The differences become apparent in the finite volume of the lattice. These HEFT predictions of the eigenstate energies are presented in fig. 2.

The left-hand plot of fig. 2 with  $m_0 = 1.7 \text{ GeV}$  illustrates the prediction of a low-lying state dominated by a single-particle quark-model-like state in the Roper regime, as indicated by the red curve from HEFT. The problem with this fit is that this single-particle-dominated state in the regime of the Roper resonance is not seen in lattice QCD. While there is a lattice QCD point on the red curve at  $\sim 1.5 \text{ GeV}$ , this state was excited by a momentum projected  $\pi N$  interpolating field [11]. It is not dominated by a three-quark operator.

The right-hand plot of fig. 2 with  $m_0 = 2.0 \text{ GeV}$  is in accord with lattice QCD results. Here the states predominantly excited by three-quark interpolating fields are associated with HEFT eigenstates with large single-particle components indicated by colour on the eigenstate energy lines.

Moreover, the composition of the scattering states predicted in HEFT with  $m_0 = 2.0 \text{ GeV}$  match the interpolating fields used to excite the states in lattice QCD. In both calculations, the lowest excitation at  $\sim 1.35 \text{ GeV}$  is dominated by  $\sigma N$  at zero back-to-back momentum and the next excitation at  $\sim 1.5 \text{ GeV}$  is dominated by  $\pi N$  with the lowest non-trivial back-to-back momentum. Table I presents a scorecard to evaluate the quality of these two HEFT descriptions.

In the valid HEFT description where  $m_0 = 2.0 \text{ GeV}$ , the  $\pi\Delta$  channel takes on an enhanced role [33] in describing the experimental  $\pi N$  phase shift and inelasticity. In this case the coupling is large and combines with  $\pi N$  and  $\sigma N$  channels to generate a pole in the complex plane. The Roper resonance arises from coupled channel rescattering in the  $\pi N$ ,  $\sigma N$  and  $\pi\Delta$  channels, the latter two being the resonant contributions of the three-body  $\pi\pi N$  contribution. This is the nature of the Roper resonance.

#### 4. – Resolution of the missing baryon resonances problem

We close by discussing the impact of the  $2s$  radial excitation of the nucleon being observed at  $1.9 \text{ GeV}$  in lattice QCD calculations near the physical point [6, 10, 11] as opposed to  $1.44 \text{ GeV}$  as anticipated historically [41, 42].

As the single-particle quark-model state is mixed with nearby two-particle states to form resonances, we anticipate the  $2s$  radial excitation is largely associated with the  $N1/2^+(1880)$  resonance observed in photoproduction and to a smaller extent the

TABLE I. – *Scorecard for the agreement between lattice QCD calculations and two HEFT descriptions of experimental  $\pi N$  scattering phase shifts and inelasticities. The  $m_0 = 2.0 \text{ GeV}$  description characterises the Roper resonance as arising from coupled channel rescattering.*

Criteria	$m_0 = 1.7 \text{ GeV}$	$m_0 = 2.0 \text{ GeV}$
Describes experimental data well and produces poles in accord with PDG.	✓	✓
1st lattice scattering state created via $\sigma N$ interpolator has dominant $\langle \sigma N   E_1 \rangle$ in HEFT.	✓	✓
2nd lattice scattering state created via $\pi N$ interpolator has dominant $\langle \pi N   E_2 \rangle$ in HEFT.	✗	✓
Lattice-QCD states excited with 3-quark interpolators are associated with HEFT states with large $\langle N_0   E_\alpha \rangle$ .	✗	✓
HEFT predicts three-quark states existing in lattice QCD.	✗	✓

TABLE II. – *Quark-model predictions [41] for the energies of the radial excitations of the nucleon and the  $\Delta$  in units of GeV are compared with contemporary lattice QCD calculations [6, 10, 43].*

State	Quark model	Lattice QCD	State	Quark model	Lattice QCD
$N1/2^+ 2s$	1.54	1.90(6)	$\Delta3/2^+ 1s$	1.23	1.26(2)
$N1/2^+ 3s$	1.77	2.60(7)	$\Delta3/2^+ 2s$	1.80	2.14(5)
$N1/2^+ 4s$	1.88	3.60(5)	$\Delta3/2^+ 3s$	1.92	3.10(17)
$N1/2^+ 5s$	1.98		$\Delta3/2^+ 4s$	1.99	

$N1/2^+(1710)$  as it is only 170 MeV away. This is supported by the right-hand plot of fig. 2 where the large single-particle basis state contributions are illustrated in colour.

In this light, it seems erroneous to tune the parameters of the quark model to place the radial excitation of the nucleon at 1440 MeV. The proliferation of radial excitations below 2 GeV is a direct consequence of this misidentification. Table II reports the predictions of the quark model [41] tuned to place the  $2s$  excitation at 1540 MeV, a little higher than the Roper resonance in anticipation of some meson-baryon dressings. These predictions for the nucleon and  $\Delta$  contrast the reality of lattice QCD calculations.

Had the quark model been tuned to place the  $2s$  excitation at 1.9 GeV, the next excitations would be well above 2 GeV. In this regard, the missing resonance problem may be regarded as further evidence that the  $2s$  radial excitation of the nucleon is not associated with the Roper resonance.

\* \* \*

This research was undertaken with the assistance of resources from the National Computational Infrastructure (NCI), and by the Phoenix HPC service at the University of Adelaide. This research was supported by the Australian Research Council through ARC Discovery Project Grants Nos. DP190102215 and DP210103706 (DBL). J-JW was supported by the National Natural Science Foundation of China under Grant Nos. 12175239 and 12221005, and by the National Key R&D Program of China under Contract No. 2020YFA0406400. Z-WL was supported by the National Natural Science Foundation of China under Grant Nos. 12175091, 11965016, 12047501, and 12247101, and the 111 Project under Grant No. B20063.

## REFERENCES

- [1] MAHBUB M. S., KAMLEH W., LEINWEBER D. B., MORAN P. J. and WILLIAMS A. G., *Phys. Lett. B*, **707** (2012) 389.
- [2] MAHBUB M. S., KAMLEH W., LEINWEBER D. B., MORAN P. J. and WILLIAMS A. G., *Phys. Rev. D*, **87** (2013) 094506.
- [3] ALEXANDROU C., LEONTIOU T., PAPANICOLAS C. N. and STILIARIS E., *Phys. Rev. D*, **91** (2015) 014506.
- [4] LEINWEBER D., KAMLEH W., KIRATIDIS A., LIU Z.-W., MAHBUB S., ROBERTS D., STOKES F., THOMAS A. W. and WU J., *JPS Conf. Proc.*, **10** (2016) 010011.
- [5] ROBERTS D. S., KAMLEH W. and LEINWEBER D. B., *Phys. Lett. B*, **725** (2013) 164.
- [6] ROBERTS D. S., KAMLEH W. and LEINWEBER D. B., *Phys. Rev. D*, **89** (2014) 074501.
- [7] KIRATIDIS A. L., KAMLEH W., LEINWEBER D. B. and OWEN B. J., *Phys. Rev. D*, **91** (2015) 094509.
- [8] KIRATIDIS A. L., KAMLEH W., LEINWEBER D. B., LIU Z.-W., STOKES F. M. and THOMAS A. W., *Phys. Rev. D*, **95** (2017) 074507.
- [9] KHAN T., RICHARDS D. and WINTER F., *Phys. Rev. D*, **104** (2021) 034503.

- [10] LIU Z.-W., KAMLEH W., LEINWEBER D. B., STOKES F. M., THOMAS A. W. and WU J.-J., *Phys. Rev. D*, **95** (2017) 034034.
- [11] LANG C. B., LESKOVEC L., PADMANATH M. and PRELOVSEK S., *Phys. Rev. D*, **95** (2017) 014510.
- [12] STOKES F. M., KAMLEH W. and LEINWEBER D. B., *Phys. Rev. D*, **102** (2020) 014507.
- [13] ROPER L. D., *Phys. Rev. Lett.*, **12** (1964) 340.
- [14] HALL J. M. M., KAMLEH W., LEINWEBER D. B., MENADUE B. J., OWEN B. J., THOMAS A. W. and YOUNG R. D., *Phys. Rev. Lett.*, **114** (2015) 132002.
- [15] HALL J. M. M., KAMLEH W., LEINWEBER D. B., MENADUE B. J., OWEN B. J. and THOMAS A. W., *Phys. Rev. D*, **95** (2017) 054510.
- [16] MOLINA R. and DÖRING M., *Phys. Rev. D*, **94** (2016) 056010; **94** (2016) 079901(Addendum).
- [17] LIU Z.-W., HALL J. M. M., LEINWEBER D. B., THOMAS A. W. and WU J.-J., *Phys. Rev. D*, **95** (2017) 014506.
- [18] BULAVA J. *et al.*, *Low-lying baryon resonances from lattice QCD*, these proceedings.
- [19] AOKI S. *et al.*, *Phys. Rev. D*, **79** (2009) 034503.
- [20] MICHAEL C., *Nucl. Phys. B*, **259** (1985) 58.
- [21] LUSCHER M. and WOLFF U., *Nucl. Phys. B*, **339** (1990) 222.
- [22] EDWARDS R. G. *et al.*, *Phys. Rev. D*, **84** (2011) 074508.
- [23] VIRGILI A., KAMLEH W. and LEINWEBER D., *Phys. Rev. D*, **101** (2020) 074504.
- [24] STOKES F. M., KAMLEH W., LEINWEBER D. B., MAHBUB M. S., MENADUE B. J. and OWEN B. J., *Phys. Rev. D*, **92** (2015) 114506.
- [25] STOKES F. M., KAMLEH W. and LEINWEBER D. B., *PoS, LATTICE 2019* (2019) 182.
- [26] ANDERSEN C. W., BULAVA J., HÖRZ B. and MORNINGSTAR C., *Phys. Rev. D*, **97** (2018) 014506.
- [27] MORNINGSTAR C. *et al.*, *PoS, LATTICE 2021* (2022) 170.
- [28] BULAVA J., HANLON A. D., HÖRZ B., MORNINGSTAR C., NICHOLSON A., ROMERO-LÓPEZ F., SKINNER S., VRANAS P. and WALKER-LOUD A., *Nucl. Phys. B*, **987** (2023) 116105.
- [29] THOMAS A. W., *Adv. Nucl. Phys.*, **13** (1984) 1.
- [30] WU J.-J., LEE T. S. H., THOMAS A. W. and YOUNG R. D., *Phys. Rev. C*, **90** (2014) 055206.
- [31] HALL J. M. M., HSU A. C. P., LEINWEBER D. B., THOMAS A. W. and YOUNG R. D., *Phys. Rev. D*, **87** (2013) 094510.
- [32] LIU Z.-W., KAMLEH W., LEINWEBER D. B., STOKES F. M., THOMAS A. W. and WU J.-J., *Phys. Rev. Lett.*, **116** (2016) 082004.
- [33] WU J.-J., LEINWEBER D. B., LIU Z.-W. and THOMAS A. W., *Phys. Rev. D*, **97** (2018) 094509.
- [34] ABELL C. D., LEINWEBER D. B., THOMAS A. W. and WU J.-J., *Phys. Rev. D*, **106** (2022) 034506.
- [35] ABELL C. D., LEINWEBER D. B., THOMAS A. W. and WU J.-J., *Ann. Phys.*, **459** (2023) 169531.
- [36] ABELL C. D., LEINWEBER D. B., LIU Z.-W., THOMAS A. W. and WU J.-J., *Phys. Rev. D*, **108** (2023) 094519.
- [37] LI Y., WU J.-J., ABELL C. D., LEINWEBER D. B. and THOMAS A. W., *Phys. Rev. D*, **101** (2020) 114501.
- [38] LI Y., WU J.-J., LEINWEBER D. B. and THOMAS A. W., *Phys. Rev. D*, **103** (2021) 094518.
- [39] BÄR O., *Phys. Rev. D*, **95** (2017) 034506.
- [40] PARTICLE DATA GROUP (WORKMAN R. L. *et al.*), *Prog. Theor. Exp. Phys.*, **2022** (2022) 083C01.
- [41] CAPSTICK S. and ROBERTS W., *Phys. Rev. D*, **47** (1993) 1994.
- [42] ISGUR N. and KARL G., *Phys. Rev. D*, **19** (1979) 2653; **23** (1981) 817(E).
- [43] HOCKLEY L., KAMLEH W., LEINWEBER D. and THOMAS A., arXiv:2312.11574 [hep-lat] (2023).